TECHNICAL REVIEW

No. 2 — 1978

Contents

The Application of the Narrow Band Spectrum Analyzer Type 2031 to the Analysis of Transient and Cyclic Phenomena

by

R. Upton and R.B. Randall

ABSTRACT

The wide range of triggering facilities available on the Norman Band Spectrum Analyzer make its use particularly applicable to the analysis of transient signals. The purpose of this article is to discuss the various ways in which the analyzer may be used to this effect, and to give practical examples of each analysis method described. The procedures given first for short transients are developed such that longer transient signals may be analyzed, and the development of such signals investigated. Finally a method is described whereby the operating cycle of a rotating machine may be divided into parts, and each part analyzed independently of the rest.

SOMMAIRE

Grace à ses nombreuses possibilités de déclenchement, l'Analyseur de spectre à bande fine est particulièrement bien adapté à l'analyse des signaux transitoires. L'objet de cet article est d'envisager les différentes façons d'utiliser l'analyseur avec de tels signaux et de donner des exemples pratiques de chacune des méthodes d'analyse décrites. Les procédures données primitivement pour des signaux transitoires de courte durée ont été développées de façon à pouvoir analyser des signaux transistoires de plus longue durée et étudier le développement de tels signaux. Enfin, on trouvera la description d'une méthode à l'aide de laquelle on pourra diviser le cycle opératoire d'une machine tournante en plusieurs parties et analyser chaque partie indépendamment du reste.

ZUSAMMENFASSUNG

Aufgrund der weitreichenden Triggermöglichkeiten des Schmalbandanalysators ist das Gerät für die Analyse transienter Signale besonders gut geeignet. Dieser Artikel setzt sich mit den verschiedenen Methoden zur Untersuchung derartiger Signale auseinander und beschreibt

entsprechende Anwendungsbeispiele aus der Praxis. Es werden zunächst Meßverfahren für kurze transiente Signale entwickelt, die sich auch für längere transiente Signale verwenden lassen, so daß Aufbau und Ablauf dieser Signale untersucht werden können. Abschließend wird eine Methode beschrieben, bei der die Umläufe einer rotierenden Maschine in Zeitabschnitte unterteilt und diese Abschnitte einzeln, d.h. unabhängig vom restlichen Umlauf analysiert werden können.

Introduction

One of the features of the Narrow Band Spectrum Analyzer Type 2031 is the flexible transient recording facility provided at its input. The purpose of this article is to discuss the various ways in which this facility may be utilized, not only in the analysis of transient signals, but also in the analysis of cyclic phenomena, e.g., in the investigation of changes in the vibration of a machine over its operating cycle.

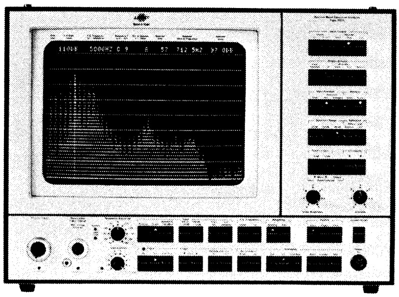

Fig. 1. Narrow Band Spectrum Analyzer Type 2031

The Narrow Band Spectrum Analyzer Type 2031 is shown in Fig.1. Briefly, it operates by sampling the input signal, and converting each sample taken into digital form. The samples are then collected into data blocks, and each data block is Fourier transformed into the frequency domain. The frequency range of the spectrum produced can be selected from 0 - 10 Hz to 0 - 20 kHz in a 1-2-5 sequence, and the sampling frequency used is always 2,56 times the full scale frequency. Since each data block consists of 1024 samples of the input signal, the duration of the data block transformed varies from 40s with a full scale frequency of 10 Hz to 20 ms when it is 20 kHz. In the analysis process, the analyzer continuously updates itself with new information, which it transforms into the frequency domain. It is when the transformation is made dependent on a trigger, however, that the analyzer becomes especially suitable for the analysis of transients.

When the 2031 is allowed to input new data continuously, it will always hold in its memory the latest 1024 samples of the input signal. If a trigger occurs, causing the transformation to take place, it will hence be the 1024 samples taken immediately prior to the time of triggering which will be transformed. (The source of the trigger could be external from an externally applied pulse, or internal from the input signal level.) However, if the start of transformation is delayed a little with respect to the trigger, the 2031 will continue to input new data during the delay, so that when transformation eventually does take place, it will be of a data block collected partly before the trigger and partly after. A longer delay, on the other hand, might mean that the data block transformed is collected entirely after the trigger.

The delay referred to above is of paramount importance in the analysis of transients in that it allows the exact data block transformed with respect to the trigger to be selected. In the 2031 it is known as the Records after Trigger setting, and it is adjustable from 0,0 to 9,9 record lengths in steps of 0,1 record length, where one record length is the time represented by 1024 samples of the input signal. A setting of, for instance, 0,5 will mean that transformation will start 0,5 record lengths after the trigger has occurred, such that the data block tranformed consists of the 512 samples taken immediately before the trigger and the 512 samples taken immediately afterwards.

For shorter transients having a duration of less than one record length, (i.e., the entire transient can be contained in less than 1024 samples of the input signal), a wide range of Records after Trigger settings is not entirely essential. In fact, (with internal triggering), settings of greater than 1,0 are rarely used, and the most common setting is 0,9, whereby 10% of the analyzed data block occurs before the trigger and 90% afterward, hence retaining a certain amount of pre-trigger information. It is in the analysis of longer transients, however, that this wide range is required. Such signals, which may have a duration of several record lengths, can often consist of several separate signals which run together, (a good example of this is punch press noise). By using a common trigger point and a variable Records after Trigger setting, it is possible with a signal such as this to index the analyzed time period along the signal and investigate the development of its various components.

Another item of importance in the use of the 2031 in the analysis of transients is the concept of transient averaging, i.e. where a shock or a transient is repetitive, an ensemble of them may be averaged in order to improve the statistical reliability of the results. It is here that the converging linear algorithm used in the 2031 becomes of benefit. This algorithm is as follows:

$$Y_n = \frac{(n-1)\ Y_{n-1} + X_n}{n}$$

where Y_n is the current average, Y_{n-1} is the previous average, and X_n is the current instantaneous value. This algorithm will always generate a true linear average of the previous n values, irrespective of the valye of n. Hence, it is no longer necessary to know the final value of n prior to starting the average. This is important since, for example, where the occurrence of the transients is uncontrolled, n might be an unknown. For a direct linear average, however, using the algorithm:

$$Y_n = \sum_{n=1}^{N} \frac{x_n}{N}$$

N must be fixed before the average takes place, and a true result is only obtained when n = N.

Measurement Technique

This section describes the use of the 2031 in the analysis of transient and cyclic phenomena. It begins by looking at the analysis of short transient signals, i.e., those having a duration of less than one record length, and which can hence be completely contained in 1024 samples of the input signal.

Analysis of Short Transient Signals

The analysis of short transient signals using the 2031 presents relatively few problems. There are, however, a couple of points to be noted, particularly with respect to the use of a weighting function. A typical analysis obtained from the 2031 is shown in Fig.3. The time function of the analyzed signal, also read out from the 2031, is shown in Fig.2. (This particular time function was produced using a mechanical frog).

In the analysis of short transients such as that of Fig.2 it should be noted that the transient itself will always limit the bandwidth of the measurement. Where the effective duration of the transient signal is T

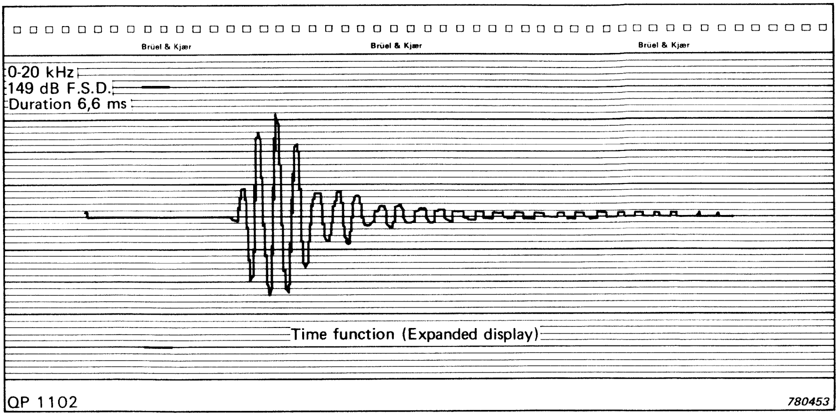

Fig. 2. Time history of a short transient produced by a mechanical frog

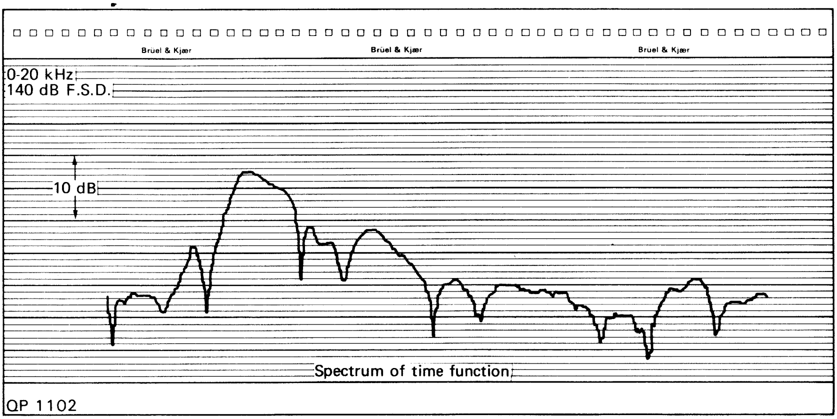

Fig. 3. Frequency spectrum of transient shown in Fig. 2

seconds, then the narrowest bandwidth possible is 1/T Hz, and hence where the measurement bandwidth of the analyzer is already less than 1/T Hz, there is no extra information to be obtained by reducing the measurement bandwidth further. In fact, reducing the measurement bandwidth (by reducing the frequency range) can actually degrade the analysis, since the duration of the data block analyzed is increased, while the duration of the transient remains the same. This not only allows the possible introduction of more extraneous noise, but also decreases the amount of transient energy per measurement bandwidth. Hence, it is a general rule that the transient should be analyzed on the highest frequency range possible where it can still be completely contained in 1024 samples of the input signal. Following this rule will also maximise the dynamic range of the measurement.

(As an illustration to the above, consider a transient analyzed in one frequency range and then again with half the frequency range. In the second analysis, the duration of the data block analyzed will be doubled and the measurement bandwidth halved with respect to the first. Looking first at the analysis of the transient, the energy of the transient with respect to the duration of the data block will be halved in the second analysis. Since the measurement bandwidth will also be halved, the level of the transient in each measurement bandwidth will drop by 6 dB. The amount of background noise will, however have been doubled, because the data block is twice as long. The noise level will hence be the same as in the first analysis).

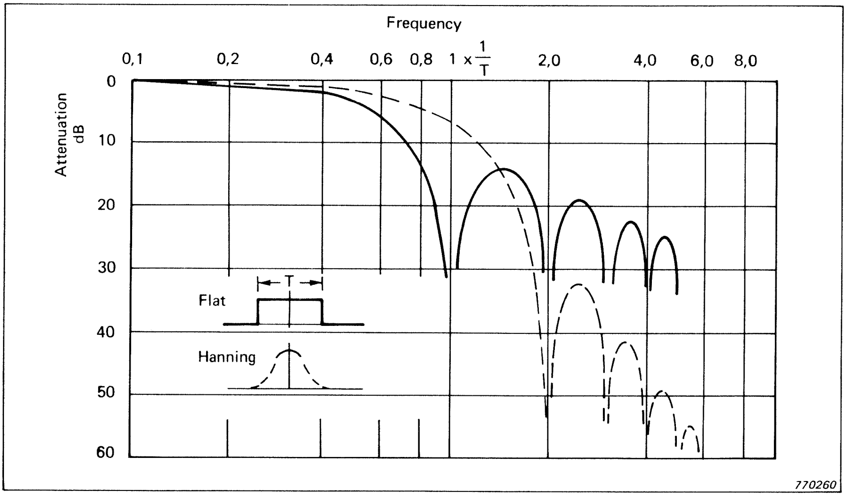

Fig. 4. Comparison of flat and Hanning Weighting functions

Regarding the question of whether a rectangular or a Hanning weighting (Fig. 4) should be used for the analysis, it should be remembered that the purpose of the Hanning weighting is to reduce to zero any signal at the ends of the data block, so as to remove discontinuities. When, however, the transient can be contained in 1024 samples of the input signal, then the ends of the data block will be at zero anyway, so use of a Hanning weighting is superfluous. Further, the Hanning weighting will actually degrade the analysis. For instance, the transient of Fig.2 was input with a Records after Trigger setting of 0,9. The curve shown in Fig.2 is of the expanded waveform, and shows only approximately the first 1/3 of the data block. Most of the energy of the transient is hence concentrated near the beginning of the data block, at a point where the Hanning weighting is reducing rapidly to zero. Use of the Hanning weighting would thus seriously alter the analyzed waveform, and again as a general rule, rectangular weighting should be used instead.

Repetitive short transients may be conveniently averaged using continuous recording and internal triggering. A linear average is started, and then each time the 2031 is triggered, the transient spectrum is automatically entered into the average. An interesting alternative to this, however, is to use manual control of the averaging process. The 2031 is set to linearly average 1 spectrum, with single recording and internal triggering. The first transient which occurs will then be entered into the average and the average will stop. The 2031 can then be rearmed to await the next transient, and when it occurs, its spectrum may be added into the average using averaging proceed, after which the average will again stop, and so on, for any number of transients. The advantage of this procedure is that prior to having its spectrum entered into

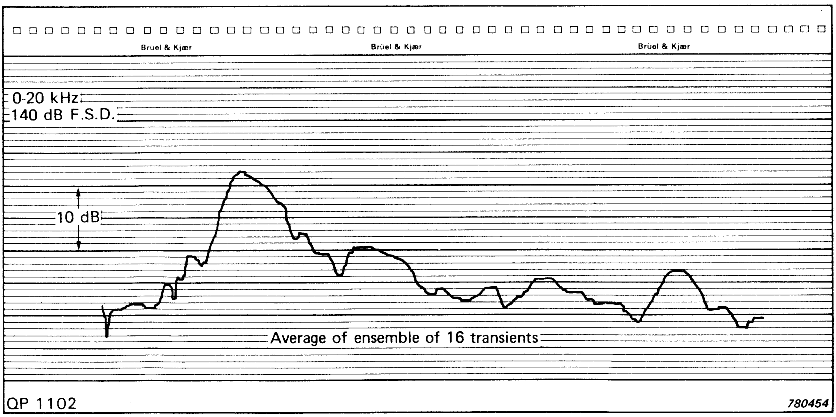

Fig.5. Average spectrum of an ensemble of 16 transients

the average, the time function of the transient can be inspected and rejected in the case of the presence, e.g., of overloads, or if the 2031 is triggered by a spurious signal, etc., so as not to degrade the average. The average is then continued until sufficient stability is obtained. An average of an ensemble of 16 transients taken in this way is shown in Fig.5. Fig.3 is one of the individual spectra making up the ensemble.

An intermediate stage between the above two types of transient analysis is to use automatic averaging as in the first type, with single recording as in the second. Then for instance, in a cycle of several signals of which only one is of interest, the 2031 can be rearmed just prior to the occurrence of the signal of interest, hence analyzing this signal and automatically entering it into the average, while ignoring the rest.

Analysis of Longer Transient Signals

As soon as a transient can no longer be contained in one data block (1024 samples in the 2031) while maintaining a sufficiently high full scale frequency, different techniques have to be used to analyze it using an FFT analyzer. These techniques, however, introduce some interesting data analysis possibilities, since they allow the development of the signal with time to be examined. Where, for instance, the signal under analysis is in reality a series of signals coming from different sources at different times, which then run together to form a longer transient, such an approach can be of particular importance.

The technique used with longer transient signals is to maintain a common trigger point and then to index the data block analyzed with respect to the trigger along the signal by using a variable Records after Trigger setting. This of course requires that the transient can be repeated either by recording it first or by repeating the process generating the transient. However, this will usually be the case, because in the cases where the transient could not be repeated easily, it would be normal measurement practice to record it when it did occur. The final item required for the analysis is some sort of gating function in order to gate out the part of the signal to be analyzed. The internal Hanning function of the 2031 fulfils this role.

The measurement technique described above was tested out using punch press noise, as this is typical of the type of signal where its use could be of benefit. The analysis was made using the system shown in Fig.6, with an Impulse Precision Sound Level Meter Type 2209 forming the input to a Digital Event Recorder Type 7502. The 7502 then re-

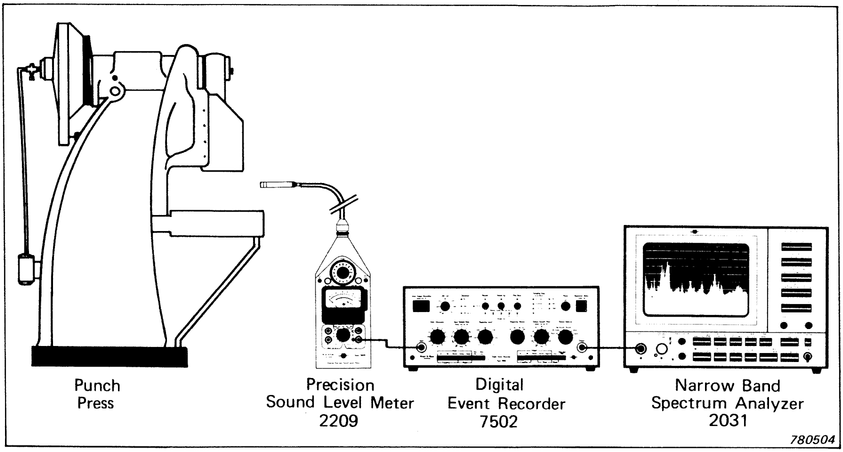

Fig. 6. Measuring Instrumentation for recording and analysis of long transient signals

cords the noise from a single cycle of the punch press, which can afterwards be repeated as often as it is necessary to the 2031 to complete the analysis.

For this technique to be effective, it is essential that the 2031 be triggered at exactly the same point in the input signal each time it is input. The most convenient way of achieving this is to use an external trigger generated from the process producing the transient itself. However, use of an internal trigger is often also possible provided that the trigger level can be adjusted with sufficient resolution. (This is usually

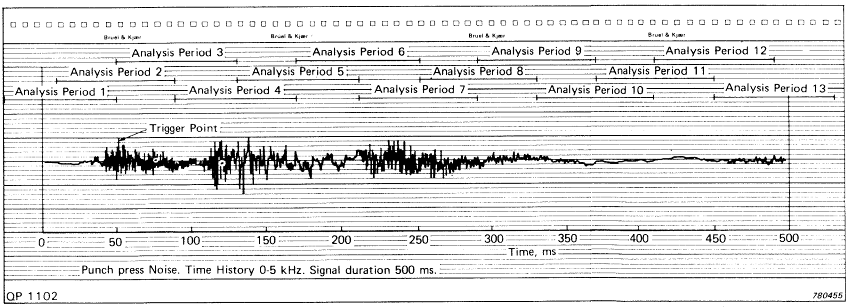

Fig. 7. Time history of a punch press noise signal (0—5 kHz)

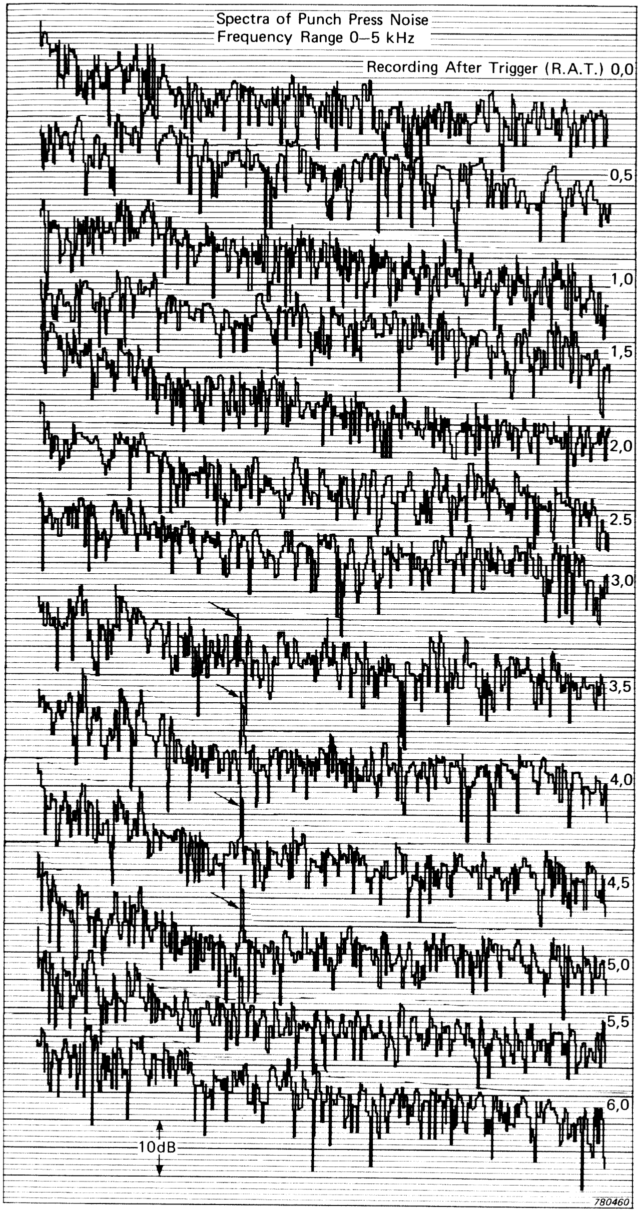

Fig.8. Spectra of analysis periods 1-13

the case with the 2031, since the trigger level is adjustable in 200 steps across the input signal level.)

The time history of a sample of punch press noise recorded on the 7502 and analyzed using the 2031 is shown in Fig.7. The signal duration is 500 ms and its upper limiting frequency is 5 kHz, (these are both functions of the 7502 control settings). A 5 kHz frequency range was hence selected on the 2031, the duration of the analyzed data block in this case being 80 ms. Internal triggering and single record were also selected, and the trigger level was set such that the 2031 would always trigger off the point shown. The analysis periods marked on Fig.7 correspond to the data blocks analyzed on the 2031, starting with a Records after Trigger setting of 0,0 for period 1, and then increasing it 0,5 record lengths at a time to obtain the analyses of periods 2-13. Note that the overlapping of the analysis periods shown is necessary, because the use of the Hanning function reduces the effective length of the data block to about 50% of its former value. Hence, although the 2031 inputs 80 ms of data, the effective length of the data is rather more like 40 ms.

The spectra obtained from analysis periods 1-13 using this technique are shown in Fig.8. Although it is difficult to draw any definite conclusions from this single measurement, (the purpose of this article is to demonstrate the measurement technique, rather than draw conclusions about the nature of punch press noise), with reference to the analysis periods marked on Fig.7, spectrum 2 could be interpreted as being

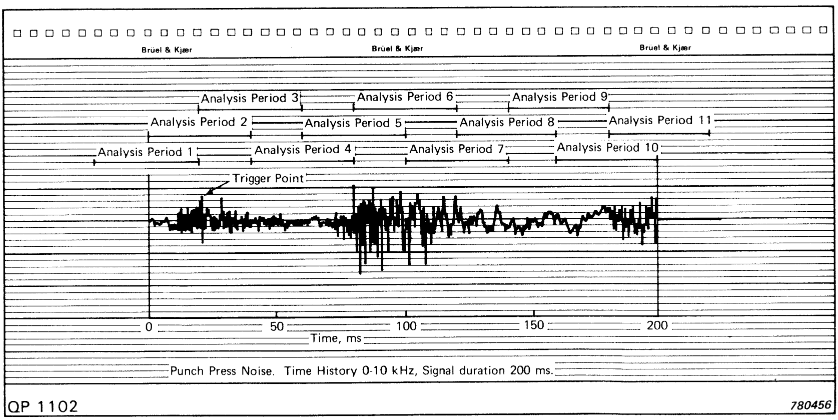

Fig.9. Time history of a punch press noise signal (0—10 kHz)

caused by the transfer of momentum from the cam to the punching tool of the press, while spectrum 4 is from the initial contact between the tool and the metal and the shearing of the metal. Spectra 6 and 7 mark the withdrawal of the punching tool, after which the metal plate being punched rings. This ringing effect can be quite clearly seen on spectra 8 through 13, as it gradually dies away.

The experiment was repeated, this time with the 7502 set to record with a 0—12,5 kHz bandwidth and the 2031 set to analyze in a frequency range of 0—10 kHz, Fig.9. It is here interesting to compare the spectra obtained from analysis periods 2 and 5, (Fig.10) i.e., the trans-

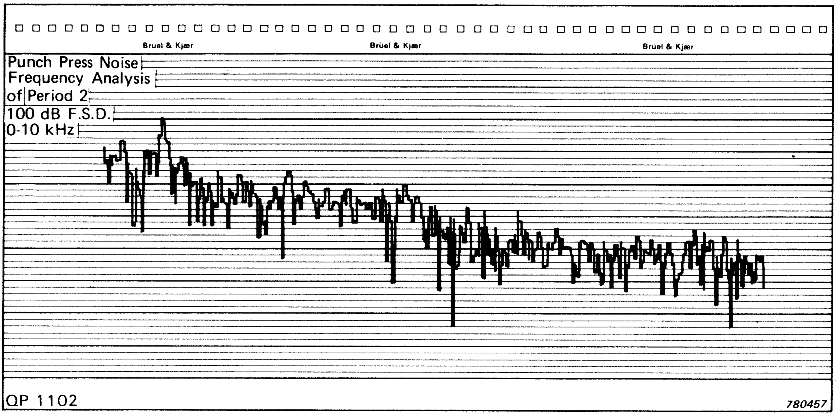

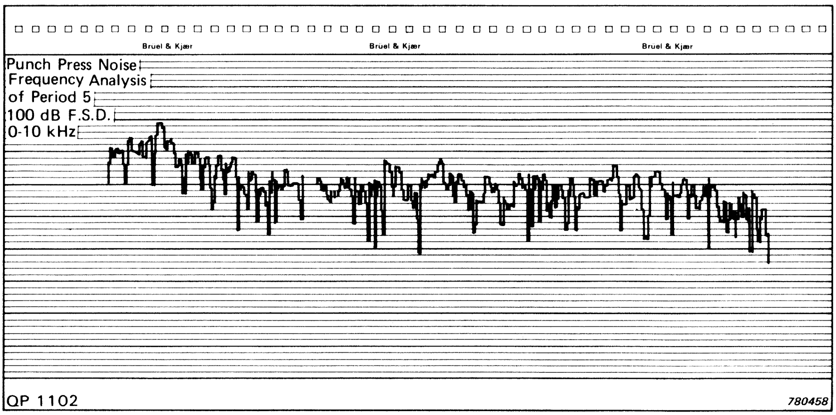

Fig.10. Spectra of analysis periods 2 and 5

fer of energy to the punching tool and the punching of the metal itsef. Spectrum 5 shows considerably higher levels than spectrum 2 at frequencies above about 5 kHz. This is an illustration of the conclusions drawn by Shinaishin, Koss & Alfredson, and Sahlin & Langé (refs. 1, 2 and 3 respectively) that it is the fracture of the metal which contributes the most to the noise emitted in a punching operation.

It is interesting to compare the time signal for each data block input by the 2031 with the original time signal output by the 7502. This time signal for analysis period 2 of the time history of Fig.7 is reproduced in Fig.11. As can be seen correspondence is very close.

The transient averaging technique described earlier can also be applied here, as long as the transient is repeatable, (e.g. for a multiple punching operation). Now, however, unless the transient has a very short rise time, use of a external trigger becomes essential. This is because it is the only way of being certain that the 2031 will always trigger at the same point in the cycle producing the transient. However, use of an external trigger with repeatable transients has one other advantage in that it makes the intermediate recording stage used in the described measurements unnecessary, i.e. the signal input can be direct to the 2031.

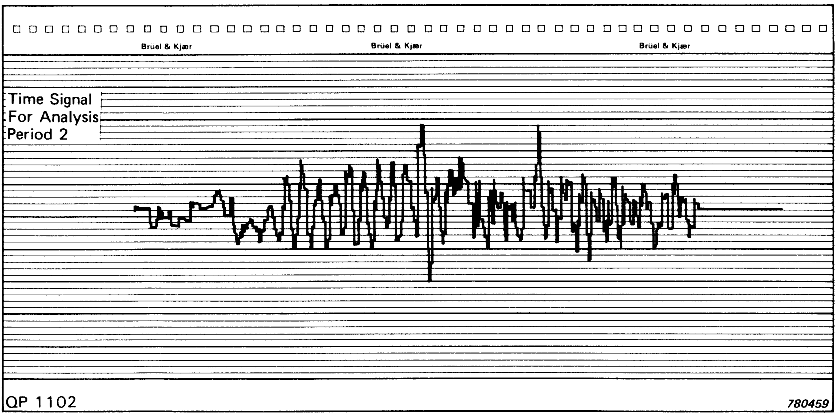

Fig.11. Time history output from 2031 of analysis period 2 of Fig.7

Analysis of Cyclic Signals

The techniques described in the previous section can also be applied to the analysis of cyclic signals, e.g., signals from rotating machines. Take, for instance, a machine rotating at 600 r.p.m., with a once per cycle tachometer pulse. One cycle of the machine will then take 100 ms. When the 2031 is set to analyze in a frequency range of 20 kHz, the data block input is 20 ms. Use of the Hanning function reduces the effective length of this data block to approximately 10 ms. Hence, by using the techometer pulse as an external trigger for the 2031, and using a variable Records after Trigger setting, the 10 ms. effective data block length analyzed by the 2031 can be moved around the cycle of the machine. As long as the tachometer signal is phase related, then changes in the spectrum can be related to events in the machine cycle, and the technique could be developed to detect effects such as, e.g., a faulty valve. Note that since the averaging techniques described earlier are still applicable, the spectrum obtained could be averaged over many machine cycles, so as to maximise the stability of the data obtained.

The proposed technique was applied to an already existing recording (complete with tachometer signal) of cylinder head vibration from a slow speed diesel engine. The motor in question (a large ship's diesel) was running at 60 r.p.m. and thus the frequency range of interest was shifted down by a decade compared with the case just mentioned. Consequently, analyses were made to 2 kHz maximum frequency. There was no particular fault with the engine in question, and in fact it was new and undergoing trials. Thus, the results could be interpreted as representing the normal condition of the engine. Moreover, the timing of the tacho signal with respect to the engine cycle is unknown, whereas in a practical case it would be known, thus allowing correlation of the various analyses with events in the engine cycle. The point to be made is that there are considerable differences between the analysis from different parts of the machine cycle, indicating that the different parts of the process are well separated from each other. A long term frequency analysis would mix with various events together, and it is quite likely that changes in one part of the cycle (e.g. a valve opening) could be completely masked by another part of the cycle (e.g. the explosion). The technique presented here would not only provide a greater likelihood of detecting changes, but also a better chance of diagnosing their case (from the part of the cycle where they occur).

The Narrow Band Analyzer Type 2031 was first used to measure the cycle time (measuring the relative time between 2 tacho pulses), and this was found to be approx. 1025 ms (i.e. about 5,1 memory lengths in the 2 kHz range). It was decided to use values of "records after trigger" from 0,0 to 5,1 in steps of 0,3 (Hanning weighting was used) and the results of doing this are reproduced in Fig.12. The overlap of 0,3 memory lengths gives a certain redundancy, but makes it easier to follow the developments. Each resulting spectrum represents an automatic linear average over 16 individual spectra, and this was found to give sufficiently repeatable results. It can be checked, for example, that the spectrum for a delay of 5,1 memory lengths (i.e. one complete cycle) is almost identical to that for 0,0, even though it was taken in a different part of the recording.

The results show that there are two main events occurring in the cycle, one fairly broadband in the vicinity of 1500 Hz, which occurs at delays between 0,6 and 1,2 and the other relatively narrow band in the vicinity of 500 Hz, occurring at delays between 2,4 and 3,3. This corresponds with the aural impression of the signal with the exception that the increase of the high frequency end at delays between 3,6 and 4,5 was also audible as a third event at a lower level.

It was pointed out by Priede and Grover (Ref. 4) that there can be considerable advantage diagnostically in examining the development of a diesel engine signal with time, and the present method combines the advantages of that with the additional diagnostic power of short term frequency analysis. The same advantages would apply to all slow speed reciprocating machines (with speeds between about 60 and 600 r.p.m.) such as compressors and hydraulic pumps. With higher speed machines (than about 600 r.p.m., or 1200 r.p.m. for 4-stroke engines) not only would the method be limited by the minimum record length (20 ms), but it would in any case become less applicable where the structural response (ringing) time becomes of the same order of time as the engine cycle time (and thus the various events not well separated in time).

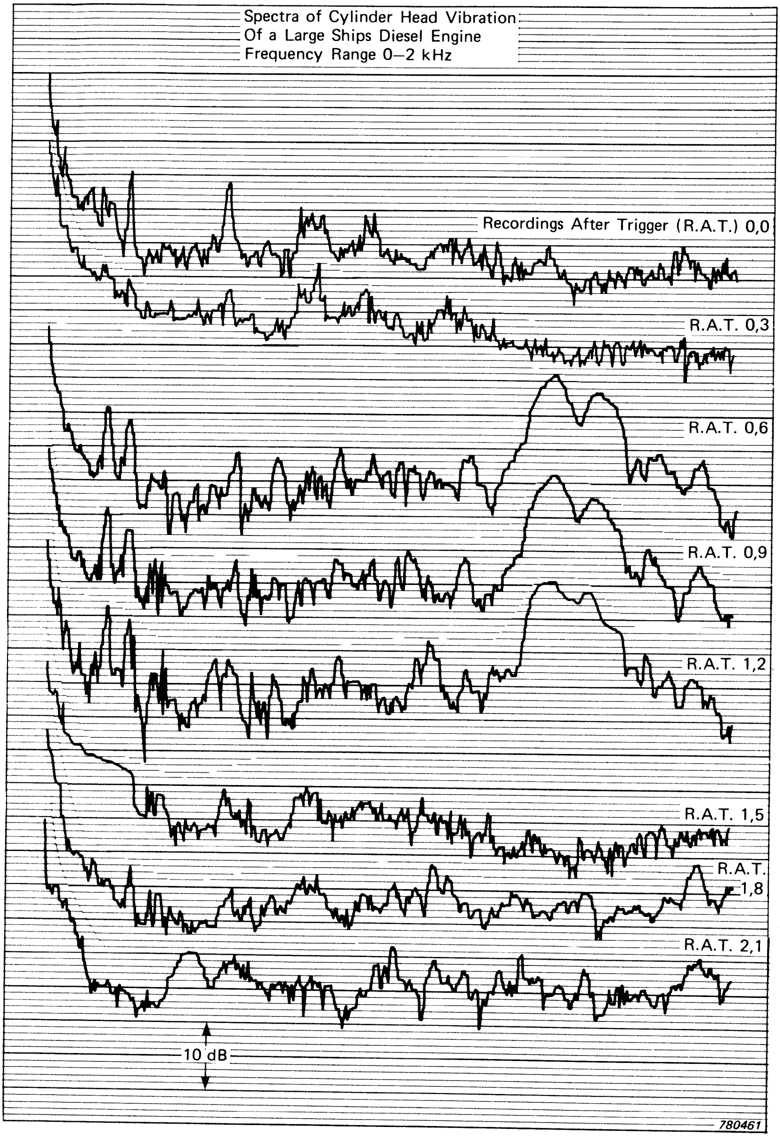

Fig. 12. Spectra of Cylinder Head vibration of a large ship's diesel engine

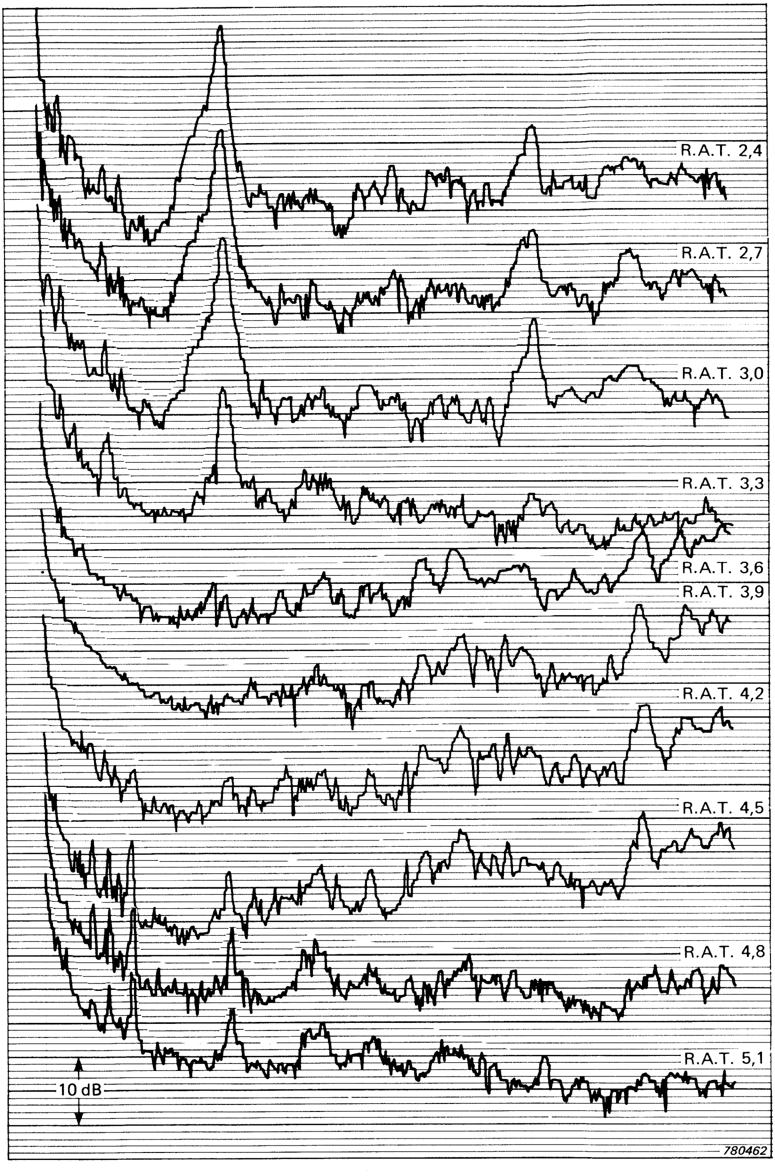

Fig. 12. Continued

References

O. SHINAISHIN: *Punch Press Noise — Outline for Analysis and Reduction* General Electric Company Technical Information Series, Report No. 72CRD103 (1972).

L. Z. KOSS & R. J. ALFREDSON: *Identification of Transient Sound Sources on a Punch Press* J. Sound Vib 34, 11—33 (1974)

S. SAHLIN & R. LANGHE: *Origins of Punch Press and Air Nozzle Noise* Noise Control Engineering 3, 3, 4—9 (1974)

PRIEDE, T. and GROVER, E.C.: *Application of Acoustic Diagnostics to Internal Combustion Engines and associated machinery*. Acoustics as a Diagnostic Tool. Institution of Mechanical Engineers, London. Meeting 20th October 1970.

Measurement of Effective Bandwidth of Filters

by

Holger Larsen

ABSTRACT

A quick and accurate method of measuring the effective bandwidth of a bandpass filter, using an integrating meter, is shown. The same technique can be used for determining the correction factors to be applied to measurement results of frequency analysis to account for any error in the effective bandwidth of a filter. Some results have been included for measurements carried out on Frequency Analyzers 1621 and 2120 used as specimens.

SOMMAIRE

On indique une méthode rapide et précise de mesure de la bande passante réelle d'un filtre passe-bande à l'aide d'un appareil de mesure intégrateur. Il est possible d'utiliser la même méthode pour déterminer les facteurs correctifs à appliquer aux résultats de mesures d'analyses de fréquence afin de tenir compte d'une éventuelle erreur dans la bande passante réelle du filtre. On a également indiqué quelques résultats de mesures réalisées sur les analyseurs de fréquence 1621 et 2120 à titre d'exemple.

ZUSAMMENFASSUNG

Es wird eine schnelle und genaue Methode zur Messung der effektiven Bandbreite mit Hilfe eines integrierenden Instruments gezeigt. Die gleiche Methode kann zur Ermittlung der Korrekturfaktoren für die Meßergebnisse hinsichtlich aller Fehler in der effektiven Bandbreite bei Frequenzanalysen benutzt werden. Für Messungen mit den Frequenzanalysatoren 1621 und 2120 als Muster werden einige Ergebnisse aufgeführt.

Introduction

In the measurement chain of instrumentation used for the frequency analysis of acoustic and vibration signals, the filter is the fundamental element. The most commonly used type of filter is the band pass filter,

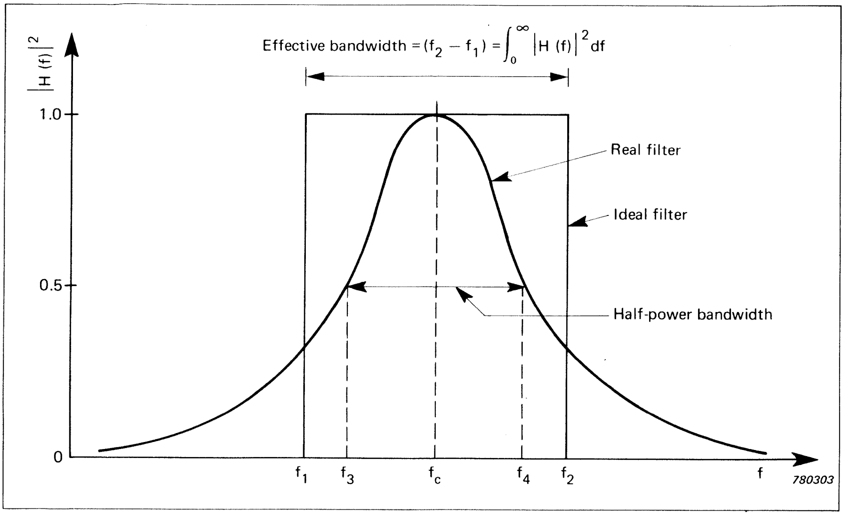

Fig. 1. Normalized Power Transfer Function of a real and an ideal filter

which ideally transmits all the frequencies within its bandwidth with zero attenuation while rejecting all the others with infinite attenuation.

Since the ideal filter, however, cannot be constructed, use has to be made of filters whose regions of transmission and attenuation are less well-defined. Fig.1 shows the normalized power transfer function $|H(f)|^2$ of a real filter [1] as a function of frequency. The bandwidth of the filter is defined here in two ways. The half power bandwidth or the so-called 3 dB bandwidth is given by

$$B_{3dB} = f_4 - f_3$$

where the power transmission of the filter is reduced to half. The effective bandwidth given by

$$B_{ea} = f_2 - f_1$$

is the bandwidth of an ideal filter that would transmit the same power as the real filter for a white noise input. To achieve this condition the area underneath the curve for the real filter should be equal to that underneath the ideal filter. The effective bandwidth is thus given by

$$B_{ea} = f_2 - f_1 = \int_0^{\infty} |H(f)|^2 df \qquad (1)$$

For a filter with ripple in its passband different reference attenuations can be defined. Fig.2 which is reproduced from IEC 561 [2] shows the power spectral density of a white noise signal sent through the real filter and through three ideal filters a, b and c. In IEC 561 the reference attenuation defined by c is used whereas IEC 225 and ANSI S1.11 1966 use definition a.

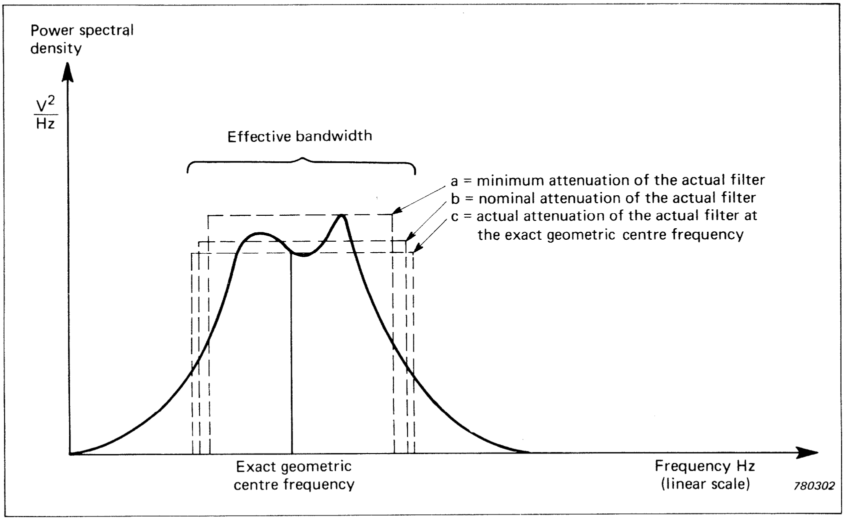

Fig.2. Various attenuation values for a filter with ripple in its passband

Conventional Methods of Bandwidth Measurements

Whilst the measurement of 3 dB bandwidth is rather simple and can be carried out with a tone generator and a voltmeter the measurement of effective bandwidth is more demanding. Traditionally it is carried out by plotting the square of the transfer function against frequency on a linear scale and measuring the area underneath the curve using a planimeter or numerical integration. The effective bandwidth is then obtained by dividing the area by the reference attenuation.

Another method involves measurement of the transfer function at equally spaced frequencies around the centre frequency and calculating the effective bandwidth from the expression

$$B_e = \frac{V_1{}^2 + V_2{}^2 + V_3{}^2 + \cdots V_n{}^2}{V_m{}^2} \times \Delta f \qquad (2)$$

where V_m is the voltage at the reference attenuation value,
$V_1, V_2 \ldots\ V_n$ are the voltages at the chosen frequencies
and Δf is the frequency spacing.

Finally, the effective bandwidth can also be determined using white or pink noise; however, this method is not as accurate.

Effective Bandwidth Measurement using an Integrating Instrument

MEASUREMENT WITH 2218

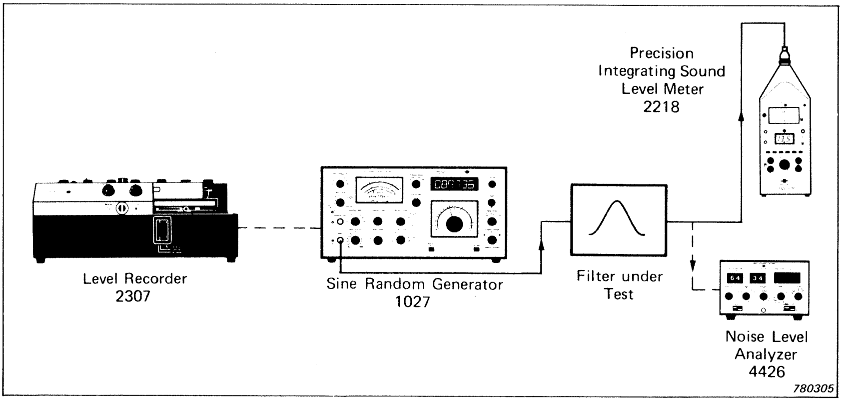

Fig.3. Instrument set-up for effective bandwidth measurement

The effective bandwidth of a filter can be measured rather simply using an L_{eq} Meter such as the Precision Integrating Sound Level Meter Type 2218. Fig.3 shows a measurement set-up in which a Sine Random Generator Type 1027 is connected to a Level Recorder Type 2307 by a Bowden cable. The measurement procedure is as follows:

1. The generator is adjusted to the frequency f_{ref} (see Fig.4) where the

reference attenuation is to be determined and an adequate voltage applied to the filter. The 2218 is started and after a suitable time T_1, the reference attenuation level L_{eqo} is read off.

2. The generator is now set to a frequency f_a (Fig.4) where the attenuation of the filter is 30 dB or more.

3. The frequency sweep of the generator and the L_{eq} measurement on the 2218 are started simulataneously. After the frequency sweep has been swept through the passband the L_{eq} measurement is stopped when the frequency f_b, where the attenuation of the filter is again 30 dB or more, is reached.

4. The L_{AX} value is now read off the 2218 and the effective bandwidth can be calculated from the formulae given below and derived in Appendix A for linear frequency sweep and in Appendix B for logarithmic frequency sweep.

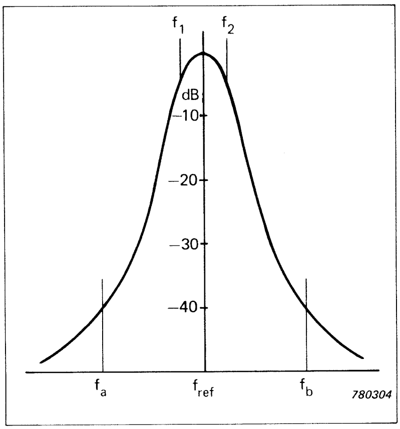

Fig.4. Characteristics of a bandpass filter

Linear Sweep
For a linear frequency sweep

$$B_{ea} = V_s T_o 10^{(L_{AX} - L_{eqo})/10} \quad [Hz] \qquad (3)$$

where T_o is a reference time of 1 s,
B_{ea} is the effective absolute bandwidth in Hz
and V_s is the sweep speed in Hz/s.

The sweep speed V_s is determined from the formula

$$V_s = \frac{100}{9} n a \qquad [Hz/s]$$

where n is the rotational speed of Drive Shaft II of Level Recorder Type 2305 or 2307 in RPM.
and a = 1 for Generator Type 1023 and
a = 0,1 1 and 10 for frequency scales 2 kHz, 20 kHz and 200 kHz respectively on Generators 1027 and 2010.

The Sweep Drive Gear of 1027 and 2010 should be in position 1/1.

Logarithmic Sweep
For a logarithmic sweep

$$B_{eo} = V_o T_o 10^{(L_{AX} - L_{eqo})/10} \qquad [octaves] \qquad (4)$$

where B_{eo} is the effective bandwidth in octaves,
V_o is the sweep speed in octaves/s,
T_o is the reference time 1 s.

The sweep speed V_o is determined from the formula

$$V_o = \frac{n}{600 \log 2} \qquad [octaves/s]$$

where n is the rotational speed of Drive Shaft II of Level Recorder Type 2305 or 2307 in RPM.

MEASUREMENT WITH 4426

When the facility for measuring L_{AX} is not available, the Noise Level Analyzer Type 4426 may be used as the integrating meter. In this case the L_{eq} value is measured during the frequency sweep as well as the sweep time T_2. The effective bandwidth can be calculated from the following formulae which are also derived in Appendix A for linear sweep and in Appendix B for logarithmic sweep.

Linear Sweep
For a linear frequency sweep

$$B_{ea} = V_s T_2 \; 10^{(L_{eq} - L_{eqo})/10} \qquad [\mathrm{Hz}] \qquad (5)$$

Logarithmic Sweep
For a logarithmic sweep

$$B_{eo} = V_o T_2 \; 10^{(L_{eq} - L_{eqo})/10} \qquad [\mathrm{octaves}] \qquad (6)$$

The symbols in equations (5) and (6) are the same as those used in equations (3) and (4).

Correction for Error in Filter Characteristics
When accurate frequency analysis measurements are to be carried out, it is important to determine the corrections to be applied to the measured results for possible errors in the effective bandwidth and the attenuation characteristics of the filter passband. The reference attenuation level (measurement of L_{eqo}) of the filter, which should be determined at the same frequency as that used for calibration of the transducer, would be common for all the filters in the spectrometer. If the spectrometer's "Linear" position is used for transducer calibration, the same should be used during measurement of the reference attenuation level.

The effective bandwidth is now measured using the same procedure as described in the previous section. The corrections for each filter are calculated according to the following formulae and should be added to the results of frequency analysis in the corresponding filter bands.

Linear Sweep

$$K_1 = 10 \log \frac{B_{na}}{B_{ea}} = \frac{B_{na}}{V_s T_o \, 10^{(L_{AX} - L_{eqo})/10}}$$

$$K_1 = 10 \log \frac{B_{na}}{V_s T_o} + L_{eqo} - L_{AX} \quad [\text{dB}] \qquad (7)$$

Where B_{na} is the nominal absolute bandwidth specified for the filter.

Logarithmic Sweep

$$K_2 = 10 \log \frac{B_{no}}{B_{eo}} = 10 \log \frac{B_{no}}{V_o T_o \; 10^{(L_{AX} - L_{eqo})/10}}$$

$$K_2 = 10 \log \frac{B_{no}}{V_o T_o} + L_{eqo} - L_{AX} \quad [\text{dB}] \qquad (8)$$

where B_{no} is the nominal bandwidth specified for the filter in octaves.

Some Practical Measurement Results

To demonstrate the method some measurements were carried out using the set-up shown in Fig.3. A Tunable Band Pass Filter Type 1621 and a Frequency Analyzer Type 2120 were chosen as measuring objects since their bandwidths are specified in terms of 3 dB bandwidths. The measurements were carried out at the centre frequency 1000 Hz with a linear frequency sweep of the generator. The results obtained are given in Table 1. The bandwidths measured are relative to the filter top and the correction factors relative to "Linear" position. As expected the effective bandwidths for 1621 and 2120 are wider than the nominal 3 dB bandwidths.

It can be seen from the formulae above that the effective bandwidth measured is directly proportional to the sweep speed which should therefore be as accurate as possible. To increase accuracy the sweep should be carried out over a wide angle of potentiometer range (of the frequency pointer). In the case of 1027 and 2010 this is achieved by choosing the lowest position on "Frequency Range" and "Frequency Scale" knobs respectively.

Analyzer Type No.	3 dB Bandwidth Nominal %	3 dB Bandwidth Measured %	Effective Bandwidth Measured %	Correction Factor K_1 dB
1621	23	22,4	31,8	– 1,4
	3	2,95	4,31	– 1,6
2120	1/3 oct.	22	22,5	0
	10	10,0	10,5	– 0,1
	3	2,79	3,4	– 0,5
	1	1,06	1,4	– 1,5

References

[1] BERANEK L: Noise and Vibration Control. McGraw-Hill Book Company 1971.

[2] IEC 561: Electro-acoustical Measuring Equipment for Aircraft Noise Certification.

[3] ASA S1.11.1966: Octave, Half-Octave, and Third-Octave Band Filter Sets.

[4] IEC 225: Octave, Half-Octave and Third-Octave Band Filters Intended for the Analysis of Sound and Vibration.

Appendix A

Linear Frequency Sweep

The reference attenuation level L_{eqo} (see Fig.4) measured by an integrating instrument is given by

$$L_{eqo} = 10 \log \frac{1}{T_1} \int_0^{T_1} \frac{(U_{ref})^2}{U_o^2} dt = 10 \log \frac{(U_{ref})^2}{U_o^2}$$

where U_{ref} is the voltage from the filter at the frequency where the reference attenuation level is required,

U_o is a reference voltage dependent on the setting of the integrating instrument,

T_1 is the measurement time.

$$\frac{(U_{ref})^2}{U_o^2} = 10^{L_{eqo}/10} \qquad \text{(A1)}$$

During the frequency sweep the L_{eq} measured is given by

$$L_{eq} = 10 \log \frac{1}{T_2} \int_0^{T_2} \frac{(U(f))^2}{U_o^2} dt \qquad \text{(A2)}$$

where $U(f)$ is the frequency dependent voltage output from the filter,

T_2 is the frequency sweep time.

For a linear frequency sweep

$$f = f_a + \frac{f_b - f_a}{T_2}\, t$$

where f_a and f_b are respectively the frequencies at which the sweep is started and stopped.

Hence $dt = T_2/(f_b - f_a)\, df$ which when substituted in A2 gives

$$L_{eq} = 10 \log \frac{1}{T_2} \int_{f_a}^{f_b} \frac{(U(f))^2}{U_o^2} \frac{T_2}{f_b - f_a}\, df = 10 \log \frac{1}{f_b - f_a} \int_{f_a}^{f_b} \frac{(U(f))^2}{U_o^2}\, df$$

$$\int_{f_a}^{f_b} \frac{(U(f))^2}{U_o^2}\, df = 10^{L_{eq}/10} (f_b - f_a) \qquad \text{(A3)}$$

The effective bandwidth B_{ea} is given by

$$B_{ea} = \int_0^{\infty} |H(f)|^2 df \qquad [\text{Hz}] \qquad \text{(A4)}$$

where H(f) is the transfer function of the filter defined by

$$H(f) = \frac{U(f)/U_o}{U_{ref}/U_o}$$

Substituting for H(f) we get

$$B_{ea} = \frac{\int_0^{\infty} \left(\frac{U(f)}{U_o}\right)^2 df}{\left(\frac{U_{ref}}{U_o}\right)^2} \approx \frac{\int_{f_a}^{f_b} \left(\frac{U(f)}{U_o}\right)^2 df}{\left(\frac{U_{ref}}{U_o}\right)^2} \qquad \text{(A5)}$$

Substituting (A1) and (A3) in (A5) we obtain

$$B_{ea} = \frac{10^{L_{eq}/10} (f_b - f_a)}{10^{L_{eqo}/10}} = (f_b - f_a)\ 10^{(L_{eq} - L_{eqo})/10} \qquad \text{(A6)}$$

Substituting sweep speed $V_s = (f_b - f_a)/T_2$ in the above equation leads to

$$B_{ea} = V_s\ T_2\ 10^{(L_{eq} - L_{eqo})/10} \qquad \text{(A7)}$$

which is given as eq.(5) in the main text and used when the integrating meter can measure the integration time T_2 such as the 4426.

Since $L_{AX} = 10 \log T_2/T_o + L_{eq}$ where $T_o = 1$ s used as a reference time

$$T_2 = T_o 10^{(L_{AX} - L_{eq})/10}$$

Substituting for T_2 in equation (A7) gives

$$B_{ea} = V_s\ T_o\ 10^{(L_{AX} - L_{eqo})/10} \qquad \text{(A8)}$$

which is given as eq.3 in the main text. This equation is used when the integrating meter has the facility for measuring L_{AX} such as the 2218.

Appendix B

Logarithmic Frequency Sweep
In the following, the same symbols are used as those used in Appendix A.

$$L_{eqo} = 10 \log \frac{1}{T_1} \int_o^{T_1} \left(\frac{U_{ref}}{U_o} \right)^2 df = 10 \log \left(\frac{U_{ref}}{U_o} \right)^2$$

i.e.

$$\left(\frac{U_{ref}}{U_o} \right)^2 = 10^{L_{eqo}/10} \qquad \text{(B1)}$$

The L_{eq} measured during frequency sweep is given by

$$L_{eq} = 10 \log \frac{1}{T_2} \int_o^{T_2} \left(\frac{U\ (f)}{U_o} \right)^2 dt \qquad \text{(B2)}$$

For a logarithmic frequency sweep

$$t = k \ln \frac{f}{f_a}$$

where k is a constant determined by setting $f = f_b$ when $t = T_2$

i.e.

$$T_2 = k \ln \frac{f_b}{f_a} \qquad \text{or} \qquad k = \frac{T_2}{\ln (f_b/f_a)}$$

Substituting for k we get

$$t = \frac{T_2}{\ln f_b/f_a} \ln f/f_a$$

Differentiating the above equation we obtain

$$dt = \frac{T_2}{\ln f_b/f_a} \frac{1}{f} df$$

Substituting for dt in eq.(B2) we obtain

$$L_{eq} = 10 \log \left[\frac{1}{T_2} \int_{f_a}^{f_b} \left(\frac{U(f)}{U_o} \right)^2 \frac{T_2}{\ln f_b/f_a} \frac{1}{f} df \right]$$

i.e.

$$L_{eq} = 10 \log \left[\frac{1}{\ln f_b/f_a} \int_{f_a}^{f_b} \left(\frac{U(f)}{U_o} \right)^2 \frac{1}{f} df \right] \qquad \text{(B3)}$$

By feeding the voltage level U_{ref} to an ideal filter and sweeping through its bandwidth $(f_2 - f_1)$ the same L_{eq} as given by (B3) would be obtained.

i.e.

$$L_{eq} = 10 \log \left[\frac{1}{\ln f_b/f_a} \int_{f_1}^{f_2} \left(\frac{U_{ref}}{U_o} \right)^2 \frac{1}{f} df \right]$$

$$= 10 \log \left[\left(\frac{U_{ref}}{U_o} \right)^2 \frac{1}{\ln f_b/f_a} \Big[\ln f \Big]_{f_1}^{f_2} \right]$$

$$L_{eq} = 10 \log \left[\left(\frac{U_{ref}}{U_o} \right)^2 \frac{\ln f_2/f_1}{\ln f_b/f_a} \right] \qquad \text{(B4)}$$

If N number of octaves are swept through the actual filter from f_a to f_b then

$$2^N = \frac{f_b}{f_a} \quad \text{i.e.} \quad N \ln 2 = \ln \frac{f_b}{f_a}$$

and the effective bandwidth B_{eo} of the ideal filter is given by

$$2^{B_{eo}} = \frac{f_2}{f_1} \quad \text{i.e.} \quad B_{eo} \ln 2 = \ln \frac{f_2}{f_1}$$

Substituting the above two equations and (B1) in (B4) we obtain

$$10^{L_{eq}/10} = 10^{L_{eqo}/10} \frac{B_{eo} \ \ln 2}{N \ \ \ln 2}$$

i.e. $$B_{eo} = N\,10^{(L_{eq} - L_{eqo})/10} \quad \text{[octaves]} \qquad \text{(B5)}$$

Eq.(B5), however, is not exact as it does not agree fully with the definition of effective bandwidth. As the sweep is logarithmic less weight is placed on the higher frequencies in the filter passband than on the lower frequencies. In other words the measurement corresponds to that when pink noise (slope —3 dB/octave) is applied to the filter instead of white noise as required by the definition. However, the error is small for normal filters with bandwidths up to 1 octave. It can be shown [3] that for an n-pole 1 octave Butterworth bandpass filter the errors are as given in the table.

n	Error in dB
2	0,07
3	0,03
4	0,014

For 1/2 octave and 1/3 octave filters the errors are even less.

The frequency sweep speed V_o [octaves/s] is given by

$$V_o T_2 = N$$

Substituting in (B5) gives

$$B_{eo} = V_o \; T_2 \; 10^{(L_{eq} - L_{eqo})/10} \tag{B6}$$

which is given as eq.(6) in the main text.

Since $L_{AX} = 10 \log \frac{T_2}{T_o} + L_{eq}$ where T_o = 1 s used as a reference time

$$T_2 = T_o \; 10^{(L_{AX} - L_{eq})/10}$$

Substituting for T_2 in equation (B6) gives

$$B_{eo} = V_o \; T_o \; 10^{(L_{AX} - L_{eqo})/10} \tag{B7}$$

which is given as eq.(4) in the main text.